Variation of tow force with velocity during offshore ploughing in granular materials

Lauder, Keith Duncan; Brown, Michael; Bransby, Mark Fraser; Gooding, Scott

Published in:
Canadian Geotechnical Journal

DOI:
10.1139/t2012-086

Publication date:
2012

Document Version
Publisher's PDF, also known as Version of record

Variation of tow force with velocity during offshore ploughing in granular materials

Keith Duncan Lauder, Michael John Brown, Mark Fraser Bransby, and Scott Gooding

Abstract: Pipeline plough behaviour has been investigated by means of reduced scale physical model testing. A testing programme was devised to investigate the influence of permeability, relative density, and plough depth on the associated tow force measured during ploughing over a range of velocities in saturated granular material. An increase in tow force with velocity was found during all of the tests and the results have been compared to previously developed analytical models. A new empirical equation has been developed to describe the change in tow force with velocity for a variety of model siliceous sand conditions. Application of this new approach to full-scale ploughing requires consideration of scaling effects and the use of appropriate input parameters determined to replicate field conditions.

Key words: pipeline ploughing, rate effects, dilation, low effective stress.

Résumé : Le comportement en labourage d'un pipeline a été étudié à l'aide d'essais réalisés sur un modèle physique à l'échelle réduite. Un programme d'essai a été élaboré dans le but d'étudier l'influence de la perméabilité, de la densité relative et de la profondeur du labourage sur la force de tire associée mesurée durant le labourage à différentes vitesses dans un matériel granulaire saturé. Une augmentation de la force de tire avec la vitesse a été observée durant tous les essais, et les résultats ont été comparés avec des modèles analytiques développés précédemment. Une nouvelle équation empirique a été développée pour décrire les changements dans la force de tire selon la vitesse, et ce pour une variété de conditions de sable de silice modélisé. L'application à l'échelle réelle de cette nouvelle approche nécessite de considérer les effets d'échelle et d'utiliser les paramètres d'entrée appropriés, qui sont déterminés dans le but de répliquer les conditions de terrain.

Mots-clés : labourage de pipeline, effets de taux, dilatation, faible contrainte effective.

[Traduit par la Rédaction]

Introduction

The oil and gas industry often buries offshore pipelines under the sea bed (cover depths $\approx$ 1.5 m are common) as this provides protection against mechanical impact, shelter against hydrodynamic loading, thermal insulation, stability under thermal expansion, and freespan mitigation (Morrow and Larkin 2007). A pipeline plough (Fig. 1) towed by a support vessel is an established method used to create a trench, often simultaneously laying the pipeline, and is favoured by the industry owing to its effectiveness in various soil conditions from very soft clays to weak rocks (Finch et al. 2000). The force (F) required to tow the plough increases with the rate of ploughing and this "rate effect" is greatest when ploughing in sands and silts due to dilation during shearing (Reece and Grinsted 1986; Palmer 1999). The tow force will ultimately affect the rate of ploughing as the support vessels that tow the plough have a limited, albeit large, towing capacity.

Prior to the commencement of any ploughing operation it is necessary to estimate the time required to complete the work as this will have a major impact on pricing and affect equipment availability of a pipeline installation contractor. This often involves the calculation of the required tow force to pull the plough at a particular depth (D) and velocity (v) through specific soil conditions. Currently much of the industry uses empirical equations to predict tow forces. The form of the equations developed has been based partially on the principle of passive lateral earth pressure and are influenced by performance data gathered during real ploughing operations (Finch et al. 2000; Cathie and Wintgens 2001). Unfortunately, where data is used from real ploughing operations there is potential for significant variation in seabed soil conditions and topography encountered (Bransby et al. 2010). Intrusive ground investigation points should be taken 0.5–1 km apart (OSIG. 2004) owing to the significant lengths of pipeline to be buried although the spacing is often far greater in practice due to time

Received 23 June 2011. Accepted 16 August 2012. Published at www.nrcresearchpress.com/cgj on 29 October 2012.

K.D. Lauder[†], M.J. Brown, and M.F. Bransby.* Civil Engineering, University of Dundee, Dundee, Scotland, DD1 4HN, UK.
S. Gooding[‡]. CTC Marine, Coniscliffe House, Coniscliffe Road, Darlington, DL3 7EE, UK.

Corresponding author: Michael John Brown (e-mail: m.j.z.brown@dundee.ac.uk).

*Present address: Advanced Geomechanics, 4 Leura Street, Nedlands, Western Australia 6009, Australia.
[†]Present address: Lloyds Register EMEA, Denburn House, 25 Union Terrace, Aberdeen, UK.
[‡]Present address: Geomarine Ltd., A2 Grainger, Prestwick Park, Newcastle upon Tyne, UK.

Fig. 1. Schematic of a typical pipeline plough during trenching.

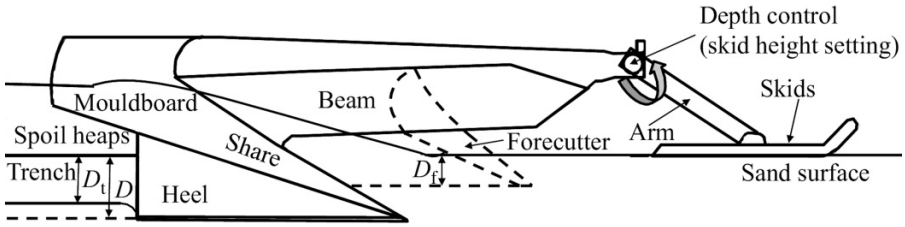

constraints and limited site investigation budget. The variability of soil conditions on any site can mean that owing to the large spacing between investigation points, the soil parameters attained from them may be unrepresentative of the material between them. This may potentially lead to inaccurate development of soil dependant parameters used in prediction models.

In contrast to the use of field data from real operations, data gathered during model ploughing tests in a laboratory environment allow both plough and soil variables to be accurately controlled and measured. Results from these tests may be used to refine existing empirical models or develop new ones. The non-rate-dependent (static) component of the tow force, which is known to comprise of interface friction and passive earth pressure components (Reece and Grinsted 1986) is now reasonably well quantified (Lauder 2011; Lauder et al. 2008). There is less confidence in the representation of the rate dependant component of tow force and the influence of soil characteristics on this dependency, for example permeability. Rate effects are known to arise from pore pressure reductions caused by water being drawn into saturated soil as it dilates under shearing (Kutter and Voss 1995). The faster the shearing event, the faster the required flow of water, which in turn requires greater pore water pressure reductions and gives rise to greater increases in effective stresses within the soil. The magnitude of pore water pressure changes at a given plough velocity will also increase with increasing drainage path length (which is typically assumed to be proportional to the plough depth, D) and reducing permeability (k) (Palmer 1999). As the rate effect is controlled by drainage of pore water fluid it will only be observed during operations, which provoke partially drained soil response, which in practice means that the tow force during ploughing will not continue to increase indefinitely with plough velocity, but will be limited when the soil response becomes fully undrained. Other phenomena that may limit the rate effect during ploughing are cavitation of pore fluid when the vapourization pressure is reached or suppression of dilation due to increased effective stresses (Kutter and Voss 1995).

Current methods that allow the prediction of rate effects

Two of the methods that can be employed to predict rate effects during offshore ploughing are those of Palmer (1999) and Cathie and Wintgens (2001). Palmer (1999) found through analytical analysis of the ploughing process that rate effects in sands and silts can be described by eq. [1].

$$[1] \qquad F_{\text{dynamic}} \propto \frac{vD^3[\Delta e/(1+e)]}{k}$$

where F_{dynamic} is the force generated with increasing rate of ploughing, v is the plough's velocity, D is the plough's depth, e is the in situ void ratio, Δe is the change in void ratio from its in situ value to that of the critical state, and k is the permeability of the soil.

In contrast, Cathie and Wintgens (2001) used a more empirical approach based upon data collected during pipeline ploughing projects to develop eq. [2], which can be used to predict the required tow force in granular soils.

$$[2] \qquad F = C_w W' + C_s \gamma' D^3 + C_d v D^2$$

where F is tow force, C_w is a friction coefficient, W' is the submerged buoyant plough weight, C_s is a passive pressure coefficient, γ' is the submerged unit weight of the soil, D is the depth from the sand surface to the share base, and C_d is a coefficient dependent on the maximum size of the smallest 10% of the particles of sand (d_{10}) and relative density (D_r).

The third term of eq. [2] gives F_{dynamic} and can be compared directly to eq. [1]. The magnitude ofC_d is assumed to increase both with relative density and with reducing d_{10}. Equation [1] is more fundamental, whereas eq. [2] is arguably of greater use for practical application by the offshore industry. Because Δe increases with relative density (above that of the critical state) and permeability increases with increasing d_{10} the main difference in the form of eqs. [1] and [2] is the exponent on the plough depth. Palmer (1999) developed eq. [1] by considering a single triangular share and assuming a vertical triangular shear zone. Cathie and Wintgens (2001) analysed data from ploughs that were fitted with a forecutter (Fig. 1), which results in the trench being formed by two separate cuts. This potentially reduces the drainage path length to the difference between the share depth and the forecutter depth for any given plough depth that is great enough to cause forecutter engagement, (drainage path length, $D_i = D - D_f$). This is assumed to be one reason why they describe the rate-dependant force as increasing with D^2 and not D^3. For this reason it is more appropriate to compare the scale model tests with eq. [1] where no forecutter was used.

This paper describes the use of reduced scale ploughing tests, conducted in a laboratory to investigate the rate dependant component of tow force (i.e., how F varies with v). The reduced scale model tests were used to investigate the influence of particle size (d_{10}) and permeability (k), relative density (D_r), and plough depth (D) on the rate dependant component of tow force. The test results are compared to an equation developed by Palmer (1999) and a new relationship for predicting rate effects in cohesionless soils during ploughing operations is developed.

Experimental techniques

The annotated schematic of a pipeline plough defines the plough depth, D, forecutter depth, D_f, and trench depth, D_t, and shows how the plough's trenching depth is controlled by rotation of the arm about the plough, which raises and lowers the skids relative to the share. The pitch of the plough is defined as the angle of the heel relative to the horizontal. Model ploughing tests were conducted at both 25th and 50th scale and the 50th scale model ploughing apparatus is shown in Fig. 2. The scale model ploughs were based on CTC Marine's Advanced Pipeline Plough, the mass of which was scaled by the cube of the scale factor and all lengths by the scale factor. The mass of the 50th scale plough was 1.6 kg in air and the mass of the 25th scale plough was 12.8 kg in air. The model ploughs were also manufactured with a detachable forecutter, which allowed its influence over plough behaviour to be investigated (Lauder et al. 2010) although all tests described herein are for ploughs without a forecutter. The 50th scale plough was connected to a carriage via a tow wire and a 20 kg capacity model RLT load cell and the whole arrangement was pulled forward by a second tow line connected to a winch. The load cell was used to measure the tow force during testing, a 200 mm stroke linear variable differential transformer (LVDT) was used to measure the plough's depth, a clinometer measured its pitch, and a draw wire transducer (DWT) measured the horizontal displacement of the carriage to allow determination of plough displacement. The use of the carriage system allowed the inclination of the tow wire to the plough to be maintained at a constant angle of 8° and also acted as a reference for plough depth measurements.

As the influence of both permeability and relative density over the rate effect was to be investigated, three sands of different grading were prepared at multiple different densities. At 50th scale, test beds were prepared by three methods (which allowed a wide range of relative densities to be achieved) in a 2 m long by 0.5 m deep by 0.5 m wide tank. The first method used was dry pluviation by a slot pluviator translated above the sand surface with a constant drop height of 800 mm. Pluviation was followed by levelling of the final surface of the sand by scraping it flat. The test bed was then saturated slowly with water through a hose attachment to the tank, which entered via a gravel base drainage layer. The level of water in the tank ensured that the plough was fully submerged throughout each test. This allowed beds to be prepared at relative densities between 90% and 50%. The second method was to pour dry sand through a funnel held just above the surface of the bed followed by scraping and saturation and resulted in very loose ($0\% < D_r < 7\%$) test beds. Medium dense beds were prepared by raking saturated sand prior to levelling. Tests were conducted in three different siliceous sands: medium sand (HST50), fine sand (HST95), and silty sand (Redhill 110) (Table 1), which were used to investigate the influence of permeability on the rate effect.

Once the test bed was prepared, the plough was placed on the surface of the sand at one end (left end in Fig. 2) of the tank and connected to the tow wire. The LVDT was then lowered onto the plough and the motor switched on to initiate the winch. The 2 m long tank gave the 250 mm long plough 1400 mm of travel, which was enough to find its steady state depth in the sand according to the plough's skid settings by moment equilibrium and provide data at the desired trenching depth. The high torque winching system allowed constant plough velocities between 20 and 200 m/h to be used in the investigation. All of the instrumentation was monitored using a USB data acquisition system with data sampling at 1 s intervals. Further information on the experimental setup and methodology is described by Lauder (2011). Sample preparation, test setup, and procedure at 25th scale was essentially the same as at 50th scale, but took place in a larger sand tank and actuation was controlled by a hydraulic system whereby a hydraulic cylinder took the place of the high torque winching system used to actuate the 50th scale plough. Further information on the 25th scale test setup can be found in Lauder (2011).

Experimental results

Figure 3 shows data gathered during three different model ploughing tests all at 50th scale. The trends are typical of all tests performed at both 25th and 50th scale. Prior to commencement of the test the plough sits on the sand, often with a shallow embedment depth although not in this case. Once forward translation is initiated the plough starts to cut deeper into the sand until it reaches a steady state whereby the depth (shaded markers, Fig. 3) and tow force (open markers, Fig. 3) are relatively constant. Steady state conditions were deemed to have developed by 600 mm forward translation of the plough for all tests. The steady state depth is determined by the plough's skid settings and by moment equilibrium acting upon the plough (Palmer et al. 1979; Lauder et al. 2008). To allow the comparison of results attained from ploughing tests, steady state forces and depths were determined by averaging all of the steady state depth and force measurements for each individual test. This gives a single value of force and a single value of depth for each of the test results presented herein.

Steady state behaviour

Figure 4 presents steady state tow forces measured during eight saturated ploughing tests at depths ranging from 37–40 mm (1.85–2.00 m at full scale) in medium-dense, medium sand (HST50) with ploughing velocities ranging from 17 to 187 m/h (model scale).

The offset of the straight line from the origin (at zero velocity) is the "static" component of the tow force ($F_{v=0}$). This can be further broken down into a passive resistance term and an interface resistance term as considered by Reece and Grinsted (1986), Cathie and Wintgens (2001), and confirmed by Lauder et al. (2008). An approximately linear relationship between tow force and velocity over the range of velocities tested is apparent. The gradient of the line fitted to the data effectively shows the magnitude of the rate effect, which is an increase of 1.85 N in tow force for every 100 m/h increase in velocity for the particular conditions (Fig. 4) and is equivalent to $1.85/11.5 = 16\%$ per 100 m/h.

Figure 5 shows plough pitch and depth plotted against velocity for the same tests as shown in Fig. 4. There appears to be a slight reduction in depth with increasing velocity of around 0.6 mm (2%) over the range of velocities tested although there is considerable scatter in the data. The plough's pitch along with the skid settings define the vertical position of the share relative to the skids and therefore the share depth (Bransby et al. 2010). There must be some skid embedment

Fig. 2. Model plough test apparatus (Lauder 2011).

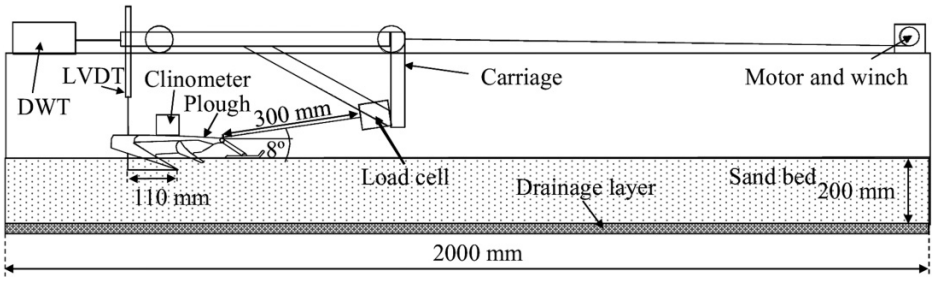

Table 1. Summary of the physical properties of the three sands tested.

Reference	Grading description	k^a (m/s)	$d_{10}{}^b$ (mm)	$d_{50}{}^c$ (mm)	ϕ'_{crit} (°)	ρ_{max} (kg/m^3)	ρ_{min} (kg/m^3)	$E'_0{}^d$ (kN/m^2)
HST50	Medium sand	4.95×10^{-4}	0.19	0.25	34	1765	1535	6500
HST95	Fine sand	1.23×10^{-4}	0.10	0.14	32	1792	1487	5000
Redhill 110	Silty sand	1.01×10^{-4}	0.08	0.12	34	1628	1295	1700

[a]Permeability shown is for each sand in a medium-dense state.
[b]Particle size at 10% percentage passing from particle-size distribution determination.
[c]Particle size at 50% percentage passing from particle-size distribution determination.
[d]One-dimensional Young's modulus is for each sand in a medium-dense state ($\sigma'_n \approx$ 5–10 kPa).

Fig. 3. Development of steady state ploughing conditions for three different tests. Tow force shown with open markers and depth with shaded markers.

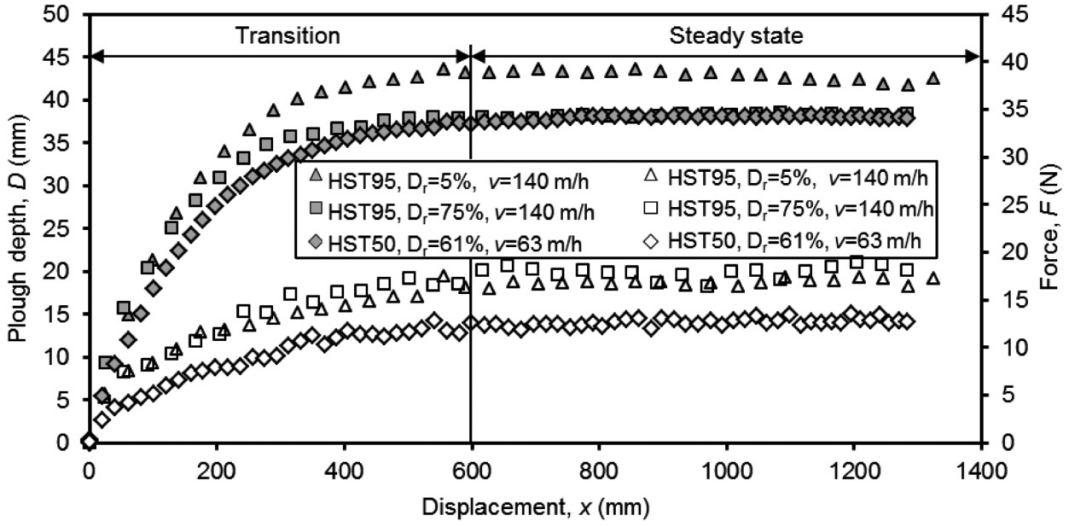

during the tests shown in Fig. 5 as there is no clear relationship between pitch and depth.

Table 2 gives a summary of all the tests described herein. The number of tests column indicates the number of tests in each series, performed at a specific set of conditions (sand type, relative density, depth, and scale). The velocity range column shows the velocity of the fastest and slowest test velocities performed within each series.

Effects of permeability

The influence of permeability on the rate effect was examined by performing saturated ploughing tests in the three different uniformly graded granular materials. Figure 6 shows steady state tow forces measured in three different sands prepared at a medium density. The grain size, d_{10} (which is often used as an indicator of permeability, e.g., Hazen 1910), and the shear characteristics of each of the three sands tested are shown in Table 1.

Rate effects are observed for all three sands in Fig. 6. The low velocity tow force is broadly the same for all of the three sands and is likely a result of them having similar relative densities and frictional properties (Table 1). The tow force achieved in the three sands diverges as ploughing velocity increases because the rate effect associated with each of the sands is different. The rate effect is greatest in the finest grained sand (Redhill110) and lowest in the coarsest (HST50) confirming that reducing permeability increases the rate effect.

Fig. 4. Variation of average steady state tow force with plough velocity in saturated medium-dense, medium sand (HST50; D_r = 61%; γ' = 9.47 kN/m³; buoyant plough weight, W' = 14.3 N; mean steady state plough depth for the test series, $\overline{D}$ = 38 mm).

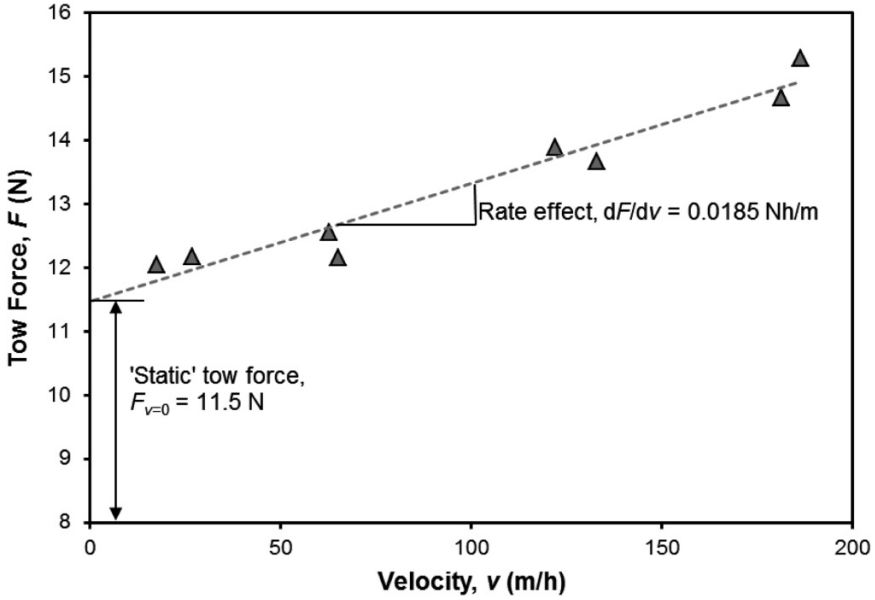

Fig. 5. The effect of plough velocity on plough depth and pitch in saturated medium-dense, medium sand (HST50; D_r = 61%; γ' = 9.47 kN/m³; buoyant plough weight, W' = 14.3 N).

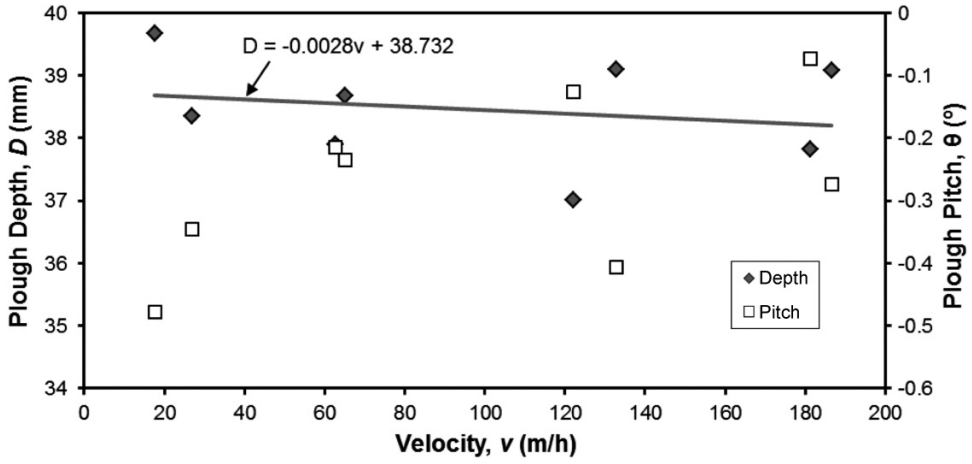

Table 2. Summary of the ploughing tests discussed.

Sand reference	D_r (%)	D (mm)	Scale	Number of tests	Velocity range (m/h)
HST95	75	40	50	9	36–472
HST95	75	65	25	4	1–334
HST95	53	39	50	14	29–383
HST95	53	65	25	8	5–334
HST95	5	43	50	3	41–191
HST95	5	38	50	3	60–192
HST50	90	36	50	6	12–183
HST50	61	39	50	8	18–187
Redhill 110	45	39	50	7	26–187

Figure 7 shows the plough depth to be most sensitive to velocity in Redhill110 and least sensitive to velocity in HST50. For the range of plough velocities investigated the plough depth reduces by approximately 12% in the Redhill110. This seems intuitive as the increased share-soil reaction would be expected to cause a change in moment equilibrium, which would alter the plough pitch and therefore its depth through the long-beam principle. Reduction in plough depth with increasing velocity then leads to an apparent reduction in the slope of the rate effect shown in Fig. 6 (i.e., the actual rate effect for the same D with increasing v would be greater than shown in Fig. 6). Thus rate effect in real ploughing operations may also lead to potential problems with depth control and the need for skid height adjustment during ploughing.

Fig. 6. Steady-state tow force variation with velocity for the three sands of different permeability.

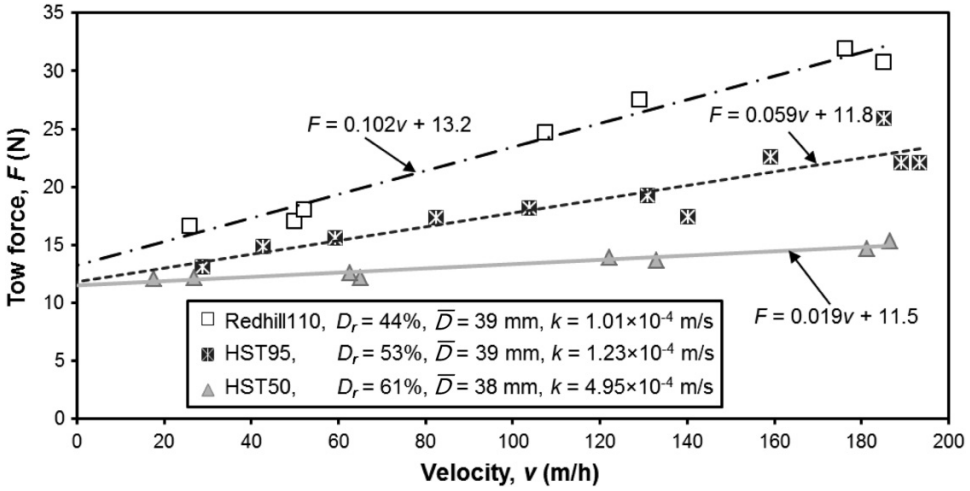

Fig. 7. Steady-state plough depth against velocity for three sands, each of different permeability.

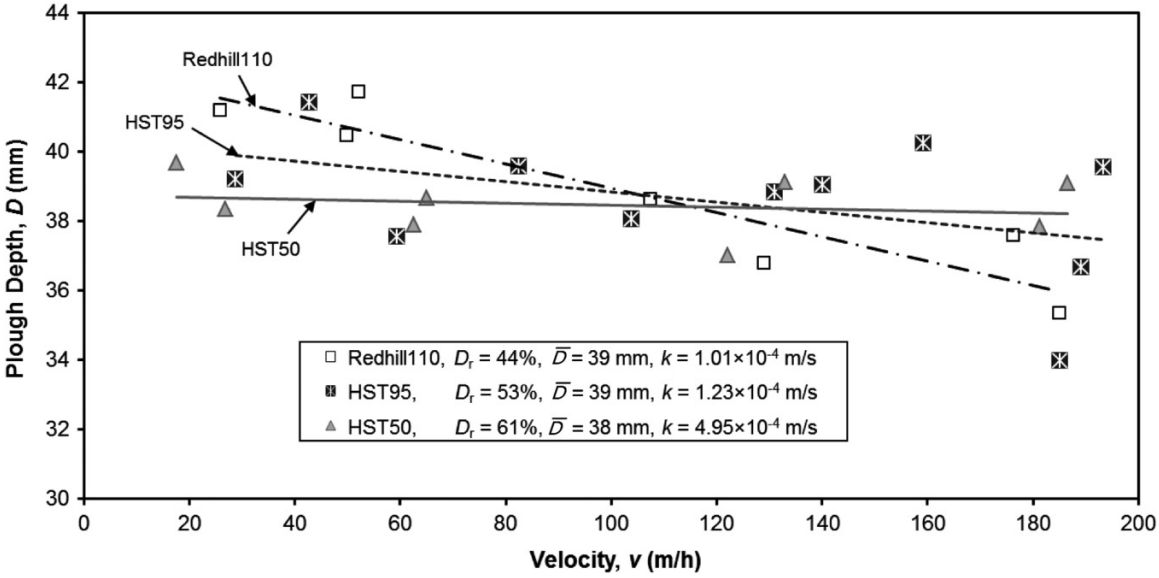

Effect of plough depth

Ploughing tests were conducted over a range of velocities at three different depths in the same fine sand (HST95) prepared at a medium density. Steady-state tow forces measured during three series of tests conducted at $\overline{D}$ = 39, 34, and 28 mm are plotted against velocity in Fig. 8.

Least squares fits to the data are presented in Fig. 8 for the three depths of ploughing with the rate effect shown as the gradient of the line, which is proven to increase with plough depth. The rate effect (i.e., the gradient of the lines, dF/dv) found for each of the three ploughing depths in Fig. 8 is plotted in Fig. 9 to find the relationship between rate effect and plough depth. Lines of rate effect proportional to D^2 and to D^3 respectfully have been fitted to the data. The results show that for a plough with a single share, the rate effect is apparently better described by being proportional to D^3 than D^2.

Effect of relative density

Ploughing tests were conducted at three values of relative density (D_r = 1%, 53%, and 75%) in saturated fine sand to investigate its effect on the tow forces generated. The plough penetrated the sand at a greater depth for the D_r = 1% test series than for the tests conducted at D_r = 53% and 75%. The trend line shown for the D_r = 1% series is a result of interpolation between six tests, three of which were conducted with $\overline{D} \approx$ 43.5 mm while the other three were conducted with $\overline{D} \approx$ 37.5 mm.

A clear rate effect is found for all three test series and can be approximated by straight lines over the range of velocities shown. The rate effect is seen to increase with relative density, which has been shown analytically by Palmer (1999). The rate effect is known to be caused by an increase in effective stresses due to pore pressure reductions caused by dilation of

Fig. 8. Influence of plough depth on the rate effect (medium dense fine sand (HST95); $W' = 14.3$ N; $\gamma' = 9.93$ kN/m^3).

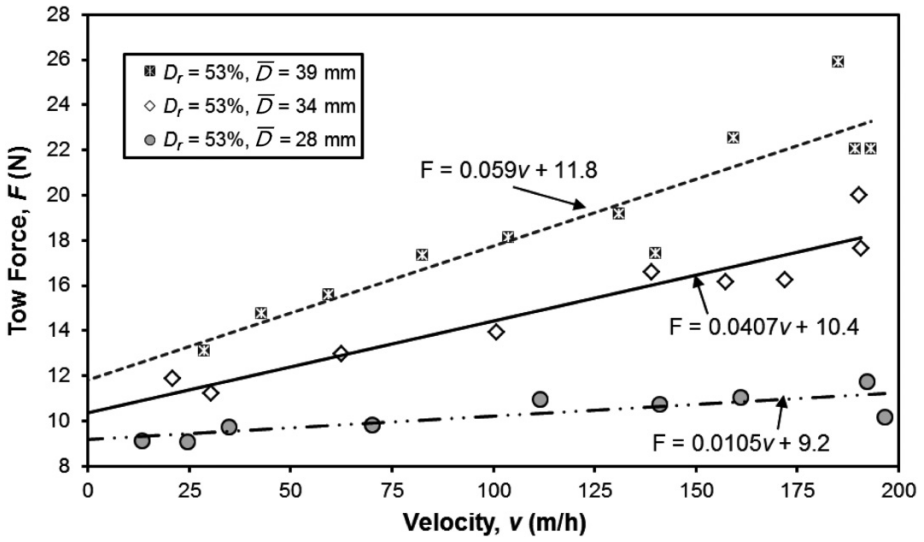

Fig. 9. Rate effect (dF/dv) measured during 50th scale tests plotted against plough depth (medium-dense, fine sand (HST95); $W' = 14.3$ N; $\gamma' = 9.93$ kN/m^3).

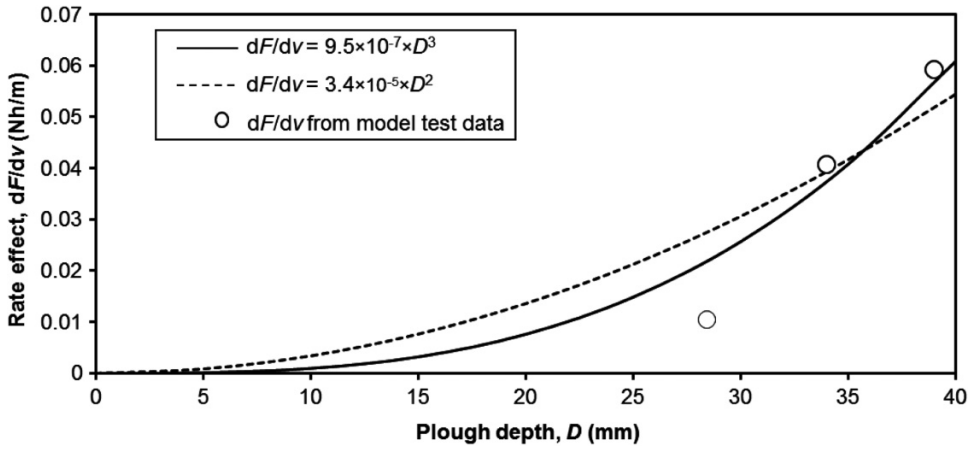

saturated sand. The reduction in pore pressure required to drive the flow into the dilating sand (and hence increase in effective stress) is dependent on the change in pore volume per unit time and the resistance to flow, which is governed by the permeability of the sand and the drainage path length. The volume change is the change in volume of the sand from its initial state to that at critical state and clearly as relative density is increased the magnitude of the rate effect will increase and is supported by the data presented in Fig. 10.

However, Fig. 10 shows that even the tests conducted in sand prepared at $D_r = 1\%$ gave a positive rate effect. This indicates that the sand is dilating, which may initially be considered surprising given the low relative density, but can be explained by the low effective stresses in the sand. At depths less than 40 mm (depth of plough during 50th scale tests) the in situ effective stresses are less than 1 kPa. Teh et al. (2006) state that the relative density at critical state is near to its loosest state ($D_r = 0\%$) at low effective stresses. Ponce and Bell (1971) found that very loose ($D_r = 5\%$) dilated at very low confining pressures (1.46 kPa) during triaxial tests. In addition, Oda and Kazama (1998) made optical measurements of shear bands on thin sections of sand cut from specimens that had been subjected to plane strain tests. They found that large voids existed within the shear band, which caused the void ratio within the shear band to exceed that of the maximum void ratio as determined by the Japanese standard method of minimum density determination. This provides some evidence that there is a possibility for even very loose sand to dilate when sheared if effective stresses are low enough.

Figure 11 shows the voids ratio during four series of direct shear box tests in HST95, which were prepared at $D_r = 1\%$, 21%, 43%, and 56%. The initial voids ratio (e_0) is the voids ratio after the normal stress was applied to the sample and e_{crit} is the voids ratio at critical state. The critical state voids ratio was found by taking global vertical displacements measured on the top loading platen of the shear box by a single LVDT during each test. It was assumed that the resulting change in voids ratio occurred over a thickness of $38d_{50}$. The assumed thickness of the dilation zone ($38d_{50}$) was selected as it caused the values of e_{crit} from tests at different e_0 to converge. It is

Fig. 10. Tow force against velocity from ploughing tests in sand of different density (saturated fine sand, d_{10} = 0.1 mm; D_r = 1%, 53%, and 75%; W' = 14.3 N; $\overline{D}$ = 40, 39, and 39.5 mm).

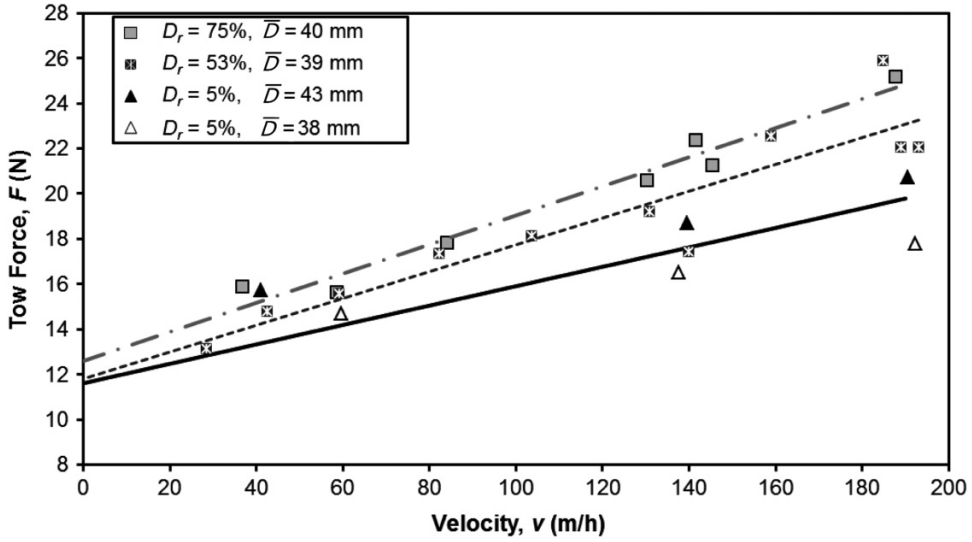

Fig. 11. Change in voids ratio from the initial state (e_0) to critical state (e_{crit}) for fine sand (HST95) during low effective stress direct shear box testing.

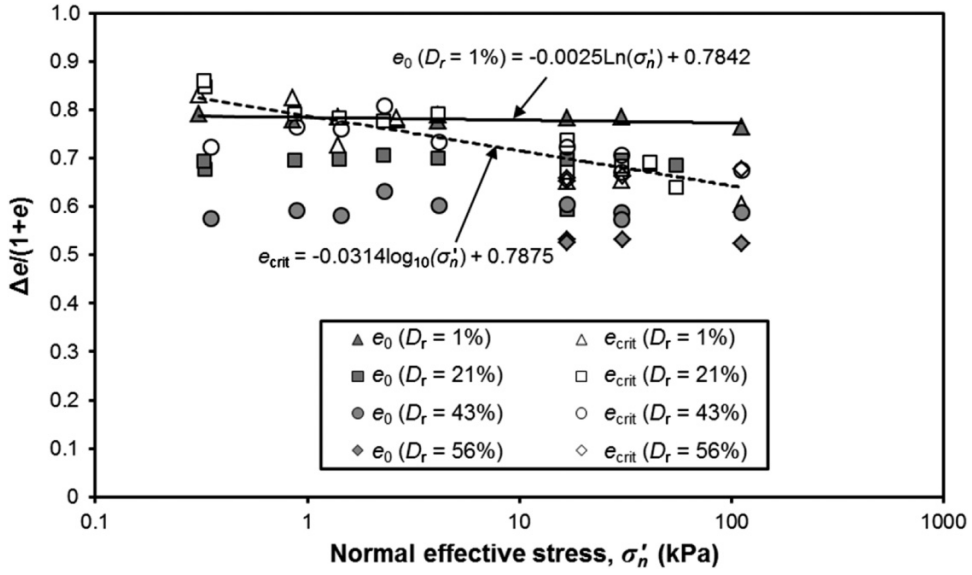

well known through observation of shear bands including those measured after shear box tests that the thickness of a shear band is somewhere between 8 and 20d_{50} thick as found by: Roscoe (1970), Mühlhaus and Vardoulakis (1987), and Finno et al. (1997). The justification for assuming volume change to occur over a greater thickness of the soil is that strains within a shear box do not occur within a single discrete shear band as shown by Potts et al. (1987) and Muir Wood (2002).

Figure 12 shows the idealized interpretation of dilation band formation within a shear box and the true expected pattern of dilation band formation within a shear box based upon examination of radiographs taken during shear box tests. In Fig. 12 the shear force is denoted Q, N is the normal force, x and y are horizontal and vertical displacements, respectively. The expected pattern (Fig. 12c) reveals that inclined shear bands are developed at each end of the box due to compression at the front of the leading edge. Therefore dilation inferred from box lid displacement (y) is a result of two shear bands and therefore the change in lid height could be due to a zone of sand 20–40d_{50} thick and can be used as a means of calculating e_{crit} from shear box tests(eq. [3]).

$$[3] \qquad e_{crit} = e_0 + \frac{\Delta H}{38 d_{50}}(1 + e_0)$$

where ΔH is the change in box lid height during shearing.

Fig. 12. (*a*) Schematic of direct shear box, (*b*) idealized interpretation of shear box, and (*c*) expected pattern of dilation bands in shear box based on radiograph observations (from Muir Wood 2002, reprinted with permission from Elsevier).

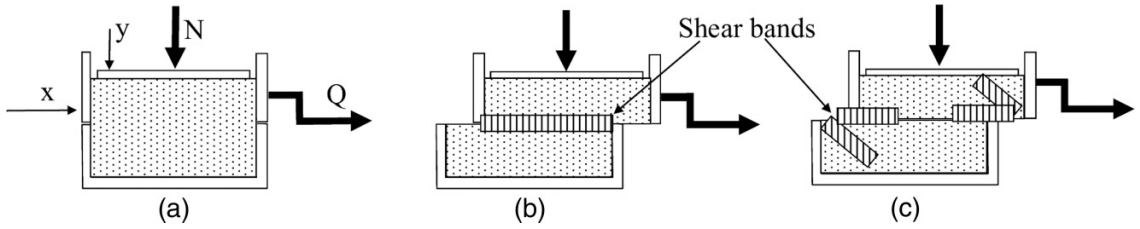

Very loose (D_r = 1%) sand was found to dilate in the shear box at very low effective stresses, which could provide an explanation as to why the ploughing tests in very loose sand show a positive rate effect. The relative density at critical state increases to around 20% at 20 kPa and therefore, if tests using a full scale plough were conducted in sand of D_r = 1%, then positive pore pressures and a reduction in effective stresses are to be expected as well. The critical state void ratio found during shear box tests can be used in the normalization of tow forces measured during ploughing tests.

Development of a general relationship to describe tow force

The results presented show that the observed rate effects (dF/dv) are linked to plough depth (D), relative density (D_r), and permeability (k). As the rate effects observed are related to certain measureable soil characteristics it is necessary to incorporate these characteristics into ploughing tow force prediction models.

Normalization of the test data shown in the results section may allow a general relationship to be developed that describes the tow force for ploughing tests at different depths in different sands at various relative densities. This may be of value to ploughing contractors as it would allow the prediction of rate effects for a wide range of conditions. Figures 13 and 14 group together data from 10 model ploughing test series at two different scales (50th and 25th) and for three different sands at various relative densities. The *y*-axes of both Figs. 13 and 14 show the rate-dependent component ($F_{dynamic} = F - F_{v=0}$) normalized by the cube of the plough's depth. The soil in front of the share is sheared during ploughing and its void ratio changes from e_0 to e_{crit}. Palmer (1999) shows that the net inflow of water per unit volume of soil associated with this change in void ratio is proportional to $\Delta e/(1 + e_0)$. Figure 13 shows plough velocity normalized by the permeability of the sand as suggested by Palmer (1999), which is valid where $vD/c_v \ll 1$. The data in Fig. 13 group reasonably well, however, there is some scatter and the series S = 50 (50th scale), HST95, D_r = 75%, D = 40 mm is noticeably to the right of the rest of the data.

A nondimensional loading rate, (eq. [4]) was proposed by Finnie (1993) during analysis of the reaction of shallow foundations subjected to vertical displacements. This has been found to pull rate effects found in different soils together (Finnie 1993) and has been applied herein.

$$[4] \qquad V = \frac{vD}{c_v}$$

where V is the normalized velocity; v is the velocity of the object penetrating the soil; D is a characteristic length taken as the diameter or width of the penetrating object, which is assumed to be analogous to the drainage path length (plough depth is used here); and c_v is the coefficient of consolidation found from the following relationship (eq. [5]):

$$[5] \qquad c_v = \frac{E_0' k}{\gamma_w}$$

where E_0' is the confined modulus, k is the permeability, and γ_w is the unit weight of water.

Therefore the nondimensional velocity, V, can be calculated by

$$[6] \qquad V = \frac{vD\gamma_w}{E_0' k}$$

In Fig. 14 the dynamic force normalized by D^3 has been plotted against the product of nondimensional velocity, V, and volume change during dilation, $\Delta e/(1 + e)$. A better agreement of the data is reached in Fig. 14 than in Fig. 13. The *x*-axis normalization in Fig. 14 is similar to that used in Fig. 13 and accounts for permeability and volume change during shearing as Fig. 13 does, but in addition accounts for the relative stiffness of the soils.

Based upon Fig. 14 a relationship has been derived (eq. [7]) to describe the rate-dependant tow force, $F_{dynamic}$ in sands.

$$[7] \qquad \frac{F - F_{v=0}}{D^3} = (6 \times 10^4)\frac{vD[\Delta e/(1 + e)]}{c_v}$$

where F and $F_{v=0}$ are forces (kN), D is depth (m), and c_v is the coefficient of consolidation (m^2/s), with $(F - F_{v=0})/D^3$ being the normalized dynamic force (kN/m^3) and 6×10^4 a coefficient (kN/m^3).

Equation [7] is valid over the range of normalized velocities presented and is not likely to continue indefinitely with increasing velocity. As previously discussed, the rate effect is caused by the partial drainage conditions that arise during ploughing. As velocity increases the conditions within the soil will eventually become fully undrained where there will be no further increase in tow force due to reducing pore pressure dissipation.

Fig. 13. Comparison of 50th and 25th scale ploughing data normalized as proposed by Palmer (1999).

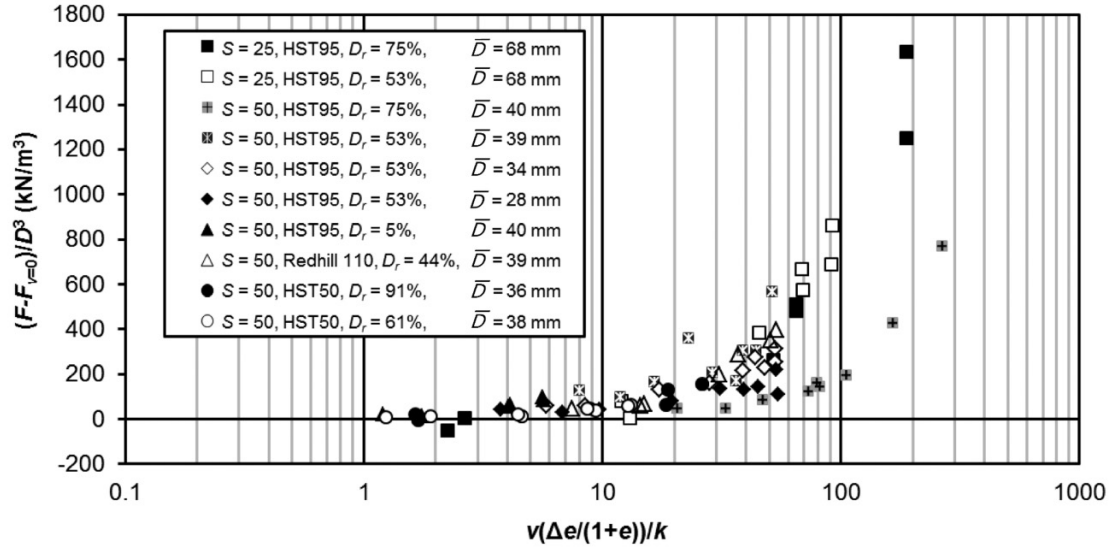

Fig. 14. Normalized tow force against normalized velocity grouping together tests for different relative densities, plough scales, plough depths, and soil types.

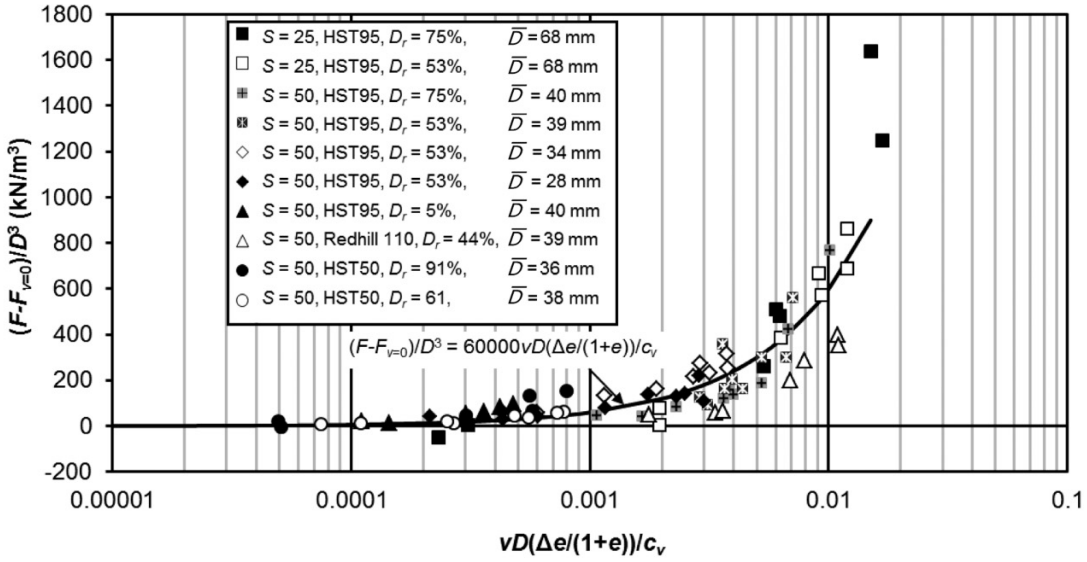

Consideration should be given to scale effects when using reduced model scale tests to predict full scale plough performance. Results from tests performed at 50th and at 25th scale are shown to compare well in Fig. 14, which may indicate that scale effects have been accounted for within the normalization. That said, there may not be enough difference between the 25th and 50th scale tests for any potential scale effects to be observed. Δe is both density and stress related and use of an appropriate value of Δe when using eq. [7] is essential for the accurate prediction of rate effects generated during full-scale ploughing. It is therefore recommended that shear box tests be performed on sand prepared at its estimated in situ relative density and eq. [3] be used to calculate e_{crit} from which the normalizing parameter $\Delta e/(1 + e)$ can be obtained.

Conclusion

Reduced scale model plough tests in carefully prepared sand beds were used to investigate the effects of soil characteristics and plough depth on the rate-dependant component of plough tow force. The test results were compared with a previously developed analytical solution and a new relationship for predicting rate effects in cohesionless soils during ploughing operations has been developed.

Analysis of reduced scale model ploughing tests reveals that the rate effect increases approximately with the cube of the

plough's depth and is presumably a result of the associated increase in drainage path lengths. This varies from the commonly adopted empirically based prediction technique (Cathie and Wintgens 2001) where it is assumed that the rate effect varies with the square of the depth.

In terms of material characteristics, the reduction in permeability associated with reducing particle size increases the magnitude of the rate effect. Additionally, increasing the relative density of the sand also increases the rate effect both due to the associated reduction in permeability and increased volume of water required to fill the dilated pores during shearing, however, its influence is perhaps not as great as one would expect.

An empirical relationship (eq. [7]) incorporating Palmer (1999) theoretical analysis of the ploughing process and the normalized velocity proposed by Finnie (1993) has been developed to determine the rate-dependent tow force during ploughing and shows good agreement with the experimental data.

As eq. [7] has been calibrated using data from reduced-scale (25th and 50th scale) ploughs its application to the prediction of rate effects during full-scale ploughing may require the consideration of scale effects. For instance, it is recommended that determination of critical voids ratio is based upon testing undertaken to mimic in situ conditions rather than those at model scale to avoid the effects of increased dilation. It should also be noted that plough depths at 50th scale are 50 times smaller than those at prototype, which reduces the resistance to flow of water through the pores of the sand. Pore fluid viscosity was not scaled (increased) during the model tests to account for this and one might expect the rate effects to be 50 times smaller than at full scale. However the agreement between the 50th and 25th scale data is in disagreement with this theory. This may be due to the product of VD plotted on the x-axis moving shallower tests with lower rate effects left and deeper tests with higher corresponding rate effects right. Palmer (1999) shows that for model tests conducted in the same soil as at prototype that if plough velocity is increased for the model by the scale factor (i.e., $V_{\text{model}}D_{\text{model}} = V_{\text{prototype}}D_{\text{prototype}}$) similar rate effects should be achieved at both scales.

Acknowledgements

Funding for this research was provided by CTC Marine Projects Ltd. and student support was provided by an Engineering & Physical Sciences Research Council (EPSRC) project grant. Technical discussions with Jim Pyrah, Julian Steward, David Cathie, and Neil Morgan are gratefully acknowledged. The views expressed are those of the authors alone at the time of writing, and do not necessarily represent the views of their respective companies.

References

Bransby, M.F., Brown, M.J., Hatherley, A.J., and Lauder, K.D. 2010. Pipeline plough performance in sand waves. Part 1: model testing. Canadian Geotechnical Journal, **47**(1): 49–64. doi:10.1139/T09-077.

Cathie, D.N., and Wintgens, J.F. 2001. Pipeline trenching using plows: performance and geotechnical hazards. *In* Proceedings of the 33rd Annual Offshore Technology Conference, Houston, Tex., 30 April – 3 May 2001. Offshore Technology Conference, Richardson, Tex. Paper No. OTC 13145. pp. 1–14.

Finch, M., Fisher, R., Palmer, A., and Baumgard, A. 2000. An integrated approach to pipeline burial in the 21st Century. *In* Proceedings of Deep Offshore Technology, New Orleans, La., November 2000.

Finnie, I.M.S. 1993. Performance of shallow foundations in calcareous soils. Ph.D. thesis, University of Western Australia, Perth, Australia.

Finno, R.J., Harris, W.W., Mooney, M.A., and Viggiani, G. 1997. Shear bands in plane strain compression of loose sand. Géotechnique, **47**: 1 149–165.

Hazen, A. 1910. Discussion of dams on sand formation. Transactions of the American Society of Civil Engineers, **73**: 199–221.

Kutter, B.L., and Voss, T. 1995. Analysis of data on plow resistance in dense, saturated, cohesionless soil. Naval Civil Engineering Laboratory, Port Hueneme, Calif., Contract Report CR 95.004.

Lauder, K.D. 2011. The performance of pipeline ploughs. Ph.D. thesis, University of Dundee, UK.

Lauder, K.D., Bransby, M.F., and Brown, M.J. 2008. Experimental testing of the performance of pipeline ploughs. *In* Proceedings of the Eighteenth International Offshore and Polar Engineering Conference, July 2008, Vancouver, B.C. pp. 212–217.

Lauder, K.D., Brown, M.J., Bransby, M.F., and Pyrah, J. 2010. Investigation into the effect of a forecutter on plough performance. *In* Proceedings of the Second International Symposium on Frontiers in Offshore Geotechnics, Perth, Australia, November 2010. pp. 865–870.

Morrow, D.R., and Larkin, P.D. 2007. The challenges of pipeline burial. *In* Proceedings of the Seventeenth (2007) International Offshore and Polar Engineering Conference, Lisbon, Portugal, 1–6 July 2007. *Edited by* E. Fontaine, F.K. Uchida, J.S. Chung, H. Moshagen, M. Sayed, and J.-W. Chen. International Society of Offshore and Polar Engineers, Cupertino, Calif. Vol. 2, pp. 900–907.

Mühlhaus, H.B., and Vardoulakis, I. 1987. The thickness of shear bands in granularmaterials. Géotechnique, **37**:(3) 271–283. doi: 10.1680/geot.1987.37.3.271.

Muir Wood, D.M. 2002. Some observations of volumetric instabilities in soils. International Journal of Solids and Structures, **39**(13–14): 3429–3449. doi:10.1016/S0020-7683(02)00166-X.

Oda, M., and Kazama, H. 1998. Microstructure of shear bands and its relation to the mechanisms of dilatancy and failure of dense granular soils. Géotechnique, **48**:(4) 465–481. doi: 10.1680/geot.1998.48.4.465.

OSIG. 2004. Guidance notes on geotechnical investigations for marine pipeline. 3rd ed. Pipeline Working Group of the Offshore Soil Investigation Forum, 10 May 2004. Society for Underwater Technology, London, UK. Available from www.sut.org.uk/pdf/pipelineguidancenotes.pdf [accessed 30 September 2012.]

Palmer, A.C. 1999. Speed effects in cutting and ploughing. Géotechnique, **49**: 3 285–294.

Palmer, A.C., Kenny, J.P., Perera, M.R., and Reece, A.R. 1979. Design and operation of an underwater pipeline trenching plough. Géotechnique, **29**:(3) 305–322. doi: 10.1680/geot.1979.29.3.305.

Ponce, V.M., and Bell, J.M. 1971. Shear strength of sand at extremely low pressures. Journal of the Soil Mechanics and Foundations Division, ASCE, **97**: 4 625–637.

Potts, D.M., Dounias, G.T., and Vaughan, P.R. 1987. Finite element analysis of the direct shear box test. Géotechnique, **37**:(1) 11–23. doi: 10.1680/geot.1987.37.1.11.

Reece, A.R., and Grinsted, T.W. 1986. Soil mechanics of submarine ploughs. *In* Proceedings of the 18th Annual Offshore Technology

Conference, Houston, Tex., 5–8 May 1986. Offshore Technology Conference, Richardson, Tex. Paper No.OTC 5341. pp. 453–461.
Roscoe, K.H. 1970. The influence of strains in soil mechanics (10th Rankine Lecture). Géotechnique, **20**:(2) 129–170. doi: 10.1680/geot.1970.20.2.129.
Teh, T.C., Palmer, A.C., Bolton, M.D., and Damgaard, J.S. 2006. Stability of submarine pipelines on liquefied seabeds. Journal of Waterway, Port, Coastal, and Ocean Engineering, **132**(4): 244–251. doi:10.1061/(ASCE)0733-950X(2006)132:4(244).

List of symbols

C_d	rate effect coefficient
C_s	passive pressure coefficient
C_w	friction coefficient
c_v	coefficient of consolidation
d_{10}	particle size at 10% percentage passing from particle-size distribution determination
d_{50}	particle size at 50% percentage passing from particle-size distribution determination
D	steady-state plough depth for an individual test
D_f	depth of forecutter engagement
D_i	drainage path length
D_{model}	plough depth at model scale
$D_{prototype}$	plough depth at prototype scale
D_r	relative density
D_t	trench depth
$\overline{D}$	mean steady-state plough depth for a test series
E_0'	confined modulus
e	void ratio
e_0	initial void ratio
e_{crit}	void ratio at critical state
Δe	change in voids ratio
F	tow force
$F_{v=0}$	tow force in fully drained conditions
$F_{dynamic}$	tow force resulting from pore pressure changes
ΔH	change in sample height (direct shearbox)
k	permeability
N	normal force (direct shearbox)
Q	shear force (direct shearbox)
S	scale factor
V	normalized velocity
V_{model}	normalized velocity at model scale
$V_{prototype}$	normalized velocity at prototype scale
v	plough velocity
W'	buoyant plough weight
γ'	effective unit weight
γ_w	unit weight of water
θ	plough pitch
ρ_{max}	maximum dry density
ρ_{min}	minimum dry density
σ_n'	normal effective stress
ϕ_{crit}'	critical state angle of friction